Journal of Thermal Analysis and Calorimetry, Vol. 90 (2007) 3, 783–793

INFLUENCE OF ALUMINIUM PRECURSOR ON PHYSICO-CHEMICAL PROPERTIES OF ALUMINIUM HYDROXIDES AND OXIDES
Part IV. $Al(OH)(CH_3COO)_2$

Barbara Pacewska[*], *Olga Kluk-Płoskońska and Dariusz Szychowski*

Warsaw University of Technology, Faculty of Building Engineering, Mechanics and Petrochemistry, Institute of Chemistry, Łukasiewicza 17 St., 09-400 Płock, Poland

The paper concerns aluminium hydroxides precipitated during hydrolysis of aluminium acetate in ammonia medium, as well as aluminium oxides obtained through their calcination at 550, 900 or 1200°C for 2 h. The following techniques were used for analysing of obtained materials: thermal analysis, IR spectroscopy, X-ray diffraction, low-temperature nitrogen adsorption, adsorption-desorption of benzene vapours and scanning electron microscopy.

Freshly precipitated boehmite/pseudoboehmite had high value of S_{BET}, very good sorption capacity for benzene vapours, developed mesoporous structure and hydrophilic character. After prolonged refluxing at elevated temperature its crystallinity increased which was accompanied by a decrease of specific surface determined from nitrogen adsorption, decrease of sorption capacity for benzene vapours and weakening of the hydrophilic character. Calcination of all hydroxides at the temperature up to 1200°C resulted in the formation of α-Al_2O_3 via transition forms of γ-, δ- and θ-Al_2O_3. The samples of aluminium oxides obtained after calcination at 550 and 900°C were characterised with high values of specific surface area and displayed quite high heat resistance, probably due to a specific morphology of starting hydroxides. The process of ageing at elevated temperature developed thermal stability of aluminium oxides.

Keywords: *acetate, boehmite, thermal decomposition, transition aluminium oxides*

Introduction

Aluminium oxides are widely prepared through thermal decomposition of aluminium hydroxides which, in turn, are conventionally obtained in the process of hydrolysis of aqueous solutions of aluminium salts with the use of such neutralising agents as $NH_3{\cdot}H_2O$, NaOH, KOH, Na_2CO_3, urea, etc. The aspect of using a particular aluminium salt involves the influence of its anionic counterpart on properties of precipitated hydroxides and final oxides. The effect of an anion present in the medium of hydrolysis has arrested some attention. Especially, ions such as SO_4^{2-}, Cl^-, and NO_3^- have been the subjects of many literature works. However, most of papers concern anion influence on physicochemical characteristic of hydroxides and only a few e.g. [1–3] discuss its role on the properties of final aluminium oxides.

With the aim to study the influence of different anions on properties of both aluminium hydroxides and oxides, five salts (chloride, nitrate, sulfate, perchlorate and acetate) were used under identical precipitation conditions employing $NH_3{\cdot}H_2O$ as the neutralising agent. The method of preparation of aluminium hydroxides and oxides was presented in the papers [4–6]. Results of investigations for chloride, perchlorate and sulfate samples have already been published [4–6].

For aluminium chloride and perchlorate containing anionic counterparts of weak affinity toward aluminium i.e. not forming stable complexes with hydrolyzed aluminium cation [4–5], the mixture of boehmite and pseudoboehmite was the product of hydrolysis; however, in the case of perchlorate, obtained precipitates displayed much higher crystallinity degree. Crystallinity of the products derived from both $AlCl_3$ and $Al(ClO_4)_3$ increased after prolonged ageing at elevated temperature. The hydroxide samples had high values of S_{BET} determined with the method of low-temperature nitrogen adsorption (234–267 and 211–262 $m^2\ g^{-1}$ for chloride and perchlorate respectively), good sorption capacity for benzene vapours and developed mesoporous structure. Aluminium hydroxides precipitated with the use of chloride salt displayed hydrophilic properties which became stronger after prolonged refluxing in mother liquor. On contrary, for aluminium perchlorate the samples had hydrophobic character which became stronger and stronger when the ageing time was longer and longer. During calcination at temperature up to 1200°C all

---

[*] Author for correspondence: ich@zto.pw.plock.pl

1388–6150/$20.00

Akadémiai Kiadó, Budapest, Hungary
Springer, Dordrecht, The Netherlands

aluminium hydroxides transformed into α-Al_2O_3 via γ, δ and θ-Al_2O_3. Transition oxides, regardless of aluminium precursor used in the hydrolysis process, were characterised with nearly equal values of specific surface (214–220 and 118–145 $m^2\ g^{-1}$ for aluminium oxides obtained from $AlCl_3$ at 550 and 900°C respectively, and 205–222 and 138–153 $m^2\ g^{-1}$ for aluminium oxides obtained from $Al(ClO_4)_3$ at 550 and 900°C respectively). The samples calcined at 1200°C displayed the lowest S_{BET} values. However, the values were a bit higher for the oxides derived from the hydroxides subjected to prolonged ageing at elevated temperature which pointed to a favourable influence of the process on thermal stability of final aluminium oxides. Moreover, the oxide samples obtained from perchlorate salt had more developed specific surface area, probably due to more advanced ageing process.

Because of a strong affinity of the SO_4^{2-} ion toward aluminium, a material freshly precipitated from aluminium sulfate was amorphous basic aluminium sulfate which after prolonged refluxing at elevated temperature in mother liquor underwent a phase transformation into highly crystalline $NH_4Al_{13}(SO_4)_2(OH)_6$ containing tridecameric unit Al_{13} [6]. It was accompanied by a decrease of specific surface area and the formation of a porous structure less accessible for benzene molecules. Regardless of the duration of the hydrolysis process, all products were characterised with poorly developed porous structure (specific surface area determined from low-temperature nitrogen adsorption: 8–19 $m^2\ g^{-1}$) and hydrophilic character. Their calcination at temperature up to 1200°C resulted in the formation of α-Al_2O_3 via transition forms of γ/η- and δ-Al_2O_3, probably without passing through θ-Al_2O_3 as opposed to the samples prepared from chloride and perchlorate. The samples of aluminium oxides obtained after calcination at 550 and 900°C had higher values of specific surface area than starting materials due to processes of dehydroxylation and desulfurization (40–79 and 88–117 $m^2\ g^{-1}$ for the oxides obtained at 550 and 900°C respectively), however much lower than the values obtained for the oxides prepared in an analogous way from $AlCl_3$ and $Al(ClO_4)_3$. The S_{BET} values calculated for the oxide samples obtained at 1200°C from aged products of hydrolysis were lower than for the analogous sample prepared without the ageing step. It was concluded that prolonged refluxing at elevated temperature of the products of hydrolysis of aluminium sulfate decreased thermal stability of final aluminium oxides, contrary to the materials derived from aluminium chloride and perchlorate.

The present paper is a further fragment of research works concerning the influence of aluminium precursor on the characteristic of aluminium hydroxides and oxides. It describes an experiment similar to cited above [4–6], nevertheless carried on with the use of aluminium acetate with the aim to study the effect of an anionic counterpart possessing some chelating ability toward aluminium cation on the properties of obtained materials.

Experimental

The products of hydrolysis of aluminium acetate were the main objects of the studies. $Al(OH)(CH_3COO)_2$ anal. grade produced by Fluka was used to prepare solutions of a desired concentration (0.5 M). Due to the fact that basic aluminium acetate is sparingly soluble in water, it was necessary to add a 36.5% solution of hydrochloric acid. The hydrolysis process was carried on in ammonia medium in exactly the same way in which the hydrolysis of other salts was conducted [4–6]. The way in which the samples of aluminium oxides were prepared are also given in papers [4–6].

Thermal analysis, IR spectroscopy and low-temperature nitrogen adsorption were conducted for all products of hydrolysis, as well as for the products of their thermal decomposition under isothermal conditions. For the hydrolysis products, both not subjected to the ageing process and aged for the longest time (59 h), as well as for aluminium oxides derived from them, additional investigations of X-ray powder diffraction and adsorption-desorption of benzene vapours were performed. The samples of the products of hydrolysis aged for 0 or 59 h and aluminium oxides prepared through their heating at 1200°C were also studied by means of scanning electron microscopy.

The TG, DTG and DTA curves were recorded using a thermoanalyser TA Instruments SDT 2960. The measurements were performed for 5–10 mg samples in air atmosphere and in a temperature range of 20–1000°C, with a heating rate of 10°C min^{-1}.

The IR spectra were accomplished by a FTIR MATSON Spectrophotometer in the wave number range of 4000–400 cm^{-1}. Powders were dispersed in a KBr matrix and pressed into thin transparent pallets.

The phase composition of the samples was determined by the X-ray diffraction method. The XRD patterns were recorded by means of a HZG-4 diffractometer (Seifert GmbH) using a Cu cathode with CuK_α radiation and a Ni filter. The measurements were performed in steps of 0.01° with pulse counting in 3 s intervals.

The degree of specific surface development was studied by volumetric determination of low-temperature nitrogen adsorption and by adsorption and desorption of benzene vapours. On the basis of obtained adsorption-desorption isotherms, by means of the programme [7], the following parameters of the porous structure were calculated: specific surface according to

BET method (S_{BET}), the surface of mesopores (S_{MEZ}) from the adsorption and desorption part of the isotherms using Kisielev method, and the distribution of mesopore surface by Dollimore-Hill method.

The morphology of the samples was determined using a scanning electron microscope (JOE, Japan).

Results and discussion

Thermal analysis

The TG, DTG and DTA curves recorded for the samples of aluminium hydroxide both not subjected to the ageing process and aged at 100°C for 59 h are presented in Figs 1a and b; whereas Table 1 reveals the values of mass loss for each step of thermal decomposition calculated for all hydroxide samples.

The thermal analysis results show that all hydroxides, regardless of the ageing process and its duration, decomposed in an analogous way.

Similarly to the products of hydrolysis of aluminium chloride and perchlorate [4, 5], the analysis of the curves evidences a two-step decomposition of the samples (Figs 1a and b) that is typical for aluminium monohydroxide (boehmite or pseudoboehmite).

In the first step ranging from 20 to 170°C, the samples lost humidity water. This endothermic effect was reflected as a peak on the DTA curve with an extremum at 57–65°C. It was accompanied by a mass loss, whose values calculated for particular samples are listed in Table 1. Comparing the values obtained for the hydroxides aged for 20, 39 or 59 h, it can be noticed that lengthening of the ageing time resulted in an increasing amount of physically adsorbed water. For the samples kept in mother liquors for 20 and 59 h the $H_2O:Al_2O_3$ ratios were 0.68 and 0.71, respectively (Table 1). Moreover, the process of ageing and lengthening of its duration, through a particle growth, probably caused a decrease of energy of water adsorption [8]. This fact was reflected in lowering of temperatures in which evaporation of physisorbed water took place; from 65°C for the hydroxide aged for 20 h to 64 and 63°C for the hydroxides aged for 39 and 59 h, respectively. Similar results were obtained for the products of hydrolysis of aluminium chloride [4].

In the second step of thermal decomposition, corresponding to the temperature range of 170–550°C, the samples received a further mass loss (Table 1).

Decomposition of boehmite takes place according to the reaction:

$$2AlO(OH) \rightarrow \gamma\text{-}Al_2O_3+H_2O$$

and is accompanied by the loss of one particle of water, which corresponds to the theoretical mass loss of

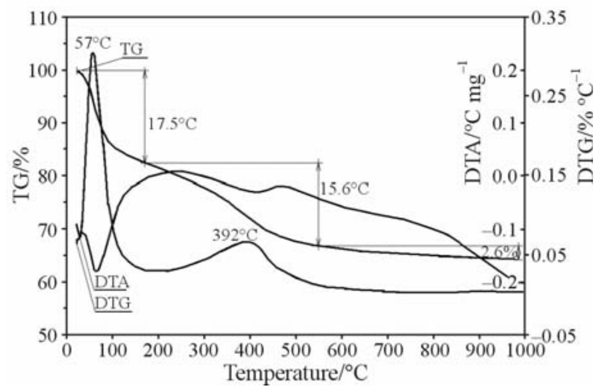

Fig. 1a TG, DTG and DTA curves for the product of hydrolysis not subjected to ageing

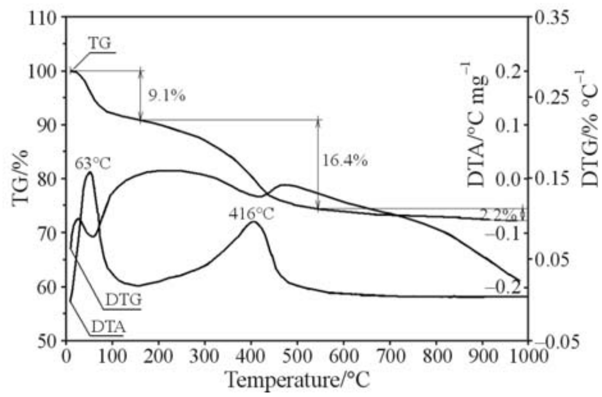

Fig. 1b TG, DTG and DTA curves for the product of hydrolysis aged for 59 h

Table 1 The mass loss values for individual steps of thermal decomposition calculated for the products of hydrolysis aged for different time intervals

Sample	Temperature range/°C					
	20–170		170–550		20–1000	
	Mass loss/%	$Al_2O_3 \cdot nH_2O$	Mass loss/%	$Al_2O_3 \cdot nH_2O$	Mass loss/%	$Al_2O_3 \cdot nH_2O$
AlOOH\0 h	17.5	1.54	15.6	1.37	35.7	3.15
AlOOH\20 h	8.6	0.68	16.6	1.30	27.9	2.19
AlOOH\39 h	8.9	0.70	17.0	1.37	28.4	2.25
AlOOH\59 h	9.1	0.71	16.4	1.29	27.7	2.17

15%. Due to the fact that the values obtained for investigated hydroxides were a bit higher than 15%, one may suppose that the samples, apart from boehmite, consisted of pseudoboehmite containing larger amount of water than boehmite.

Except the hydroxide kept in the mother liquor for 39 h, the values of mass loss were lower for aged hydroxides in comparison with this obtained for the sample obtained without the ageing step. Thus, it may be supposed that hydroxides subjected to the process of ageing for different time intervals contained less pseudoboehmite, and more boehmite, than the sample prepared without this stage. The process of ageing carried on in mother liquor and at elevated temperature probably favoured the formation of crystal structure of boehmite due to more advanced processes of condensation and dehydration of gels. In consequence, structural defects were removed and the structure became more ordered. The analogous remark was also made in papers [4, 5, 9]. The process of the removal of structural water was reflected on the DTA curve as an endothermic effect with an extremum ranging from 392 to 416°C. As it may be noticed, the temperature was higher and higher as the ageing time was longer and longer. For the sample of freshly precipitated hydroxide it was 392°C, while for the hydroxides aged for 20, 39 or 59 h it was 407, 409 and 416°C, respectively. Thus, it was concluded that the process of ageing proceeded with a particle growth up to reaching the grain size providing thermal stability that is revealed in an increase of dehydroxylation temperature.

FTIR spectroscopy

Figure 2a represents the IR spectra recorded for the products of hydrolysis of aluminium acetate in ammonia medium not subjected to ageing and aged for 59 h, whereas Fig. 2b shows the IR spectra for the products of calcination of not aged aluminium hydroxide at 550, 900 or 1200°C for 2 h.

As for the samples prepared from aluminium chloride and perchlorate [4, 5], the IR spectra of aluminium hydroxide and the products of its calcination at 550, 900 or 1200°C prepared from aluminium acetate without the ageing step are similar to the respective IR spectra recorded for analogous samples derived from aluminium hydroxides aged for different time intervals.

In the spectra of all hydroxides, there is a broad band at the wave number range of 3700–2900 cm^{-1} ascribed to the stretching vibrations of OH groups in the hydroxide structure, as well as in water physically adsorbed [10]. Within this band, another weaker one is observed at about 3029 cm^{-1} characteristic of stretching vibrations of OH groups in boehmite/pseudoboehmite structure [11, 12] (there is no distinct difference between the IR spectra of boehmite and pseudoboehmite except the intensity of peaks which is stronger for boehmite). A weakly visible band for the deformation vibrations of this group is identified at 1155 cm^{-1} [13]. The band at 900 cm^{-1} is due to the vibrational modes localised in the surface layer and it most likely reflects the deformation of surface OH groups in γ-AlOOH [14]. The presence of boehmite/pseudoboehmite in the samples is also confirmed with a very intensive peak ~1070 cm^{-1} [14] ascribed to the Al–O vibrational mode [15, 16], as well as a broad band at the wave number range of 480–750 cm^{-1}, consisted of three peaks: 741, 610 and 490 cm^{-1}, attributed to ‘condensed’ AlO_6 octahedra. As in the case of the hydroxides obtained from other aluminium precursors [4, 5], the intensity of peaks ascribed to boehmite was stronger for the samples aged in mother liquor at elevated temperature with respect to the hydroxide not subjected to ageing (compare the spectra in Fig. 2a). It confirms a suggestion made on the basis of the results of thermal analysis on a favourable influence of the ageing process on the for-

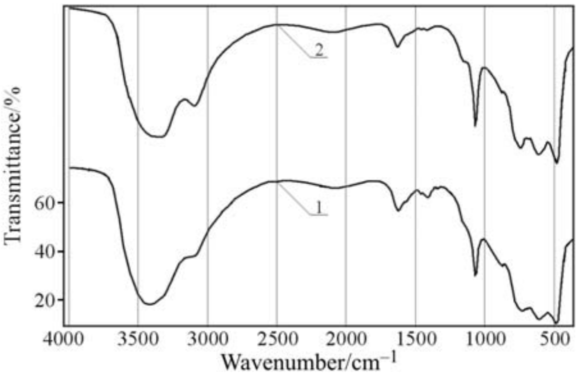

Fig. 2a IR spectra of the products of hydrolysis aged for 0 and 59 h, 1– AlOOH\0 h, 2 – AlOOH\59 h

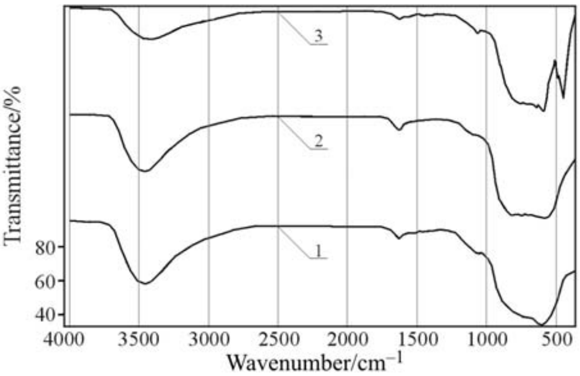

Fig. 2b IR spectra of the products of calcination of the sample AlOOH\0 h at 550, 900 and 1200°C for 2 h, 1 – AlOOH\0 h\550°C, 2 – AlOOH\0 h\550°C\900°C, 3 – AlOOH\0 h\550°C\1200°C

mation of boehmite structure. It may evidence that acetate anion disturbs the process of structural rearrangements leading to the formation of characteristic corrugated boehmite sheets only in a slight degree. Moreover, in aqueous medium, the CH_3COO^- ion is bound in a weakly dissociated molecule of acetic acid (dissociation constant $K=1.8\cdot10^{-5}$), which additionally hinders its interaction with precipitated aluminium hydroxide and makes the course of structural rearrangement easier.

In the IR spectra of hydroxides aged for different time intervals (20, 39 or 59 h) any distinct differences in the intensity of peaks characteristic of boehmite are visible, which points to small influence of ageing time on the formation of boehmite structure.

Except above mentioned bands, in the IR spectra of all hydroxides there are peaks at 1410 and 1640 cm^{-1} ascribed to the vibrations of OH groups in structural water [17, 18]. Near these bands there may be weakly visible peaks (1410 and 1553 cm^{-1}) that most likely involve residual acetate anions [19].

As for the hydroxides obtained from aluminium chloride and perchlorate [4, 5], also for the hydroxides prepared from acetate salt, the process of calcination at 550°C for 2 h led to the formation of γ-Al_2O_3 (Fig. 2b). It is confirmed by a strong broad absorption band in the region 750–900 cm^{-1}, due to the stretching vibrations of a lattice of interlinked tetrahedra AlO_4 [14]. Within this band, a peak at about 610 cm^{-1} typical of γ-Al_2O_3 [14] is observed. An increase of calcination temperature up to 900°C probably resulted in the obtainment of transition oxides of higher crystalline order. This is reflected in the character change of the band at 750–900 cm^{-1} that becomes broader, stronger and partly resolved into several sharp components of small intensity. A comparison of the spectra of these samples with literature data allows thinking that they contained δ-Al_2O_3 [14]. Simultaneously, the band in the range of 3700–2900 cm^{-1} attributed to the stretching vibrations of OH groups in the hydroxide structure, as well as in physically adsorbed water, becomes weaker. The intensity of this band is still weaker in the IR spectra of the samples calcined at 1200°C. Moreover, the character of the broad band at 750–900 cm^{-1} corresponding to the Al–O modes in the lattice also changes. In the IR spectra, new peaks at 465, 610 and 645 cm^{-1} appear which are due to vibrations of 'condensed' AlO_6 octahedra in α-Al_2O_3. Their intensity is weaker for the oxides prepared from aged hydroxides in comparison with the sample derived from the hydroxide not subjected to ageing; however, it hardly changes with lengthening of ageing time from 20 to 59 h. It evidences the fact that the process of ageing of aluminium hydroxides favoured a delayed transformation of γ-Al_2O_3 obtained from them into α phase. This is in agreement with the results for the samples prepared from aluminium chloride and perchlorate [4, 5].

A character change of the IR spectra recorded for all examined aluminium hydroxides and the products of their calcination at 550, 900 or 1200°C confirms the following sequence of phase transitions that accompanied the heating of the samples:

$$\text{Boehmite / Pseudoboehmite} \rightarrow \gamma\text{-}Al_2O_3 \rightarrow \delta\text{-}Al_2O_3 \rightarrow \theta\text{- / }\alpha\text{-}Al_2O_3$$

X-ray powder diffraction

Figure 3a represents the XRD patterns recorded for the samples of aluminium hydroxides, both not subjected to the ageing process and aged for 59 h, Fig. 3b shows the roentgenograms of the products of calcination at 550 and 900°C of not aged aluminium hydroxide, while Fig. 3c presents the X-ray patterns of aluminium oxides obtained through calcination at 1200°C of aluminium hydroxides kept in mother liquor for 0 or 59 h.

The XRD patterns obtained for the samples prepared without the ageing step are very close to analo-

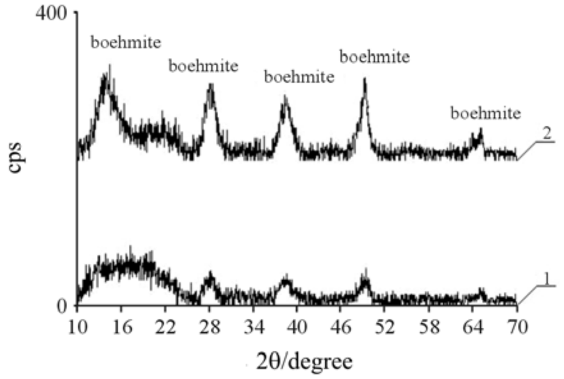

Fig. 3a XRD patterns of the products of hydrolysis aged for 0 and 59 h, 1 – AlOOH\0 h, 2 – AlOOH\59 h

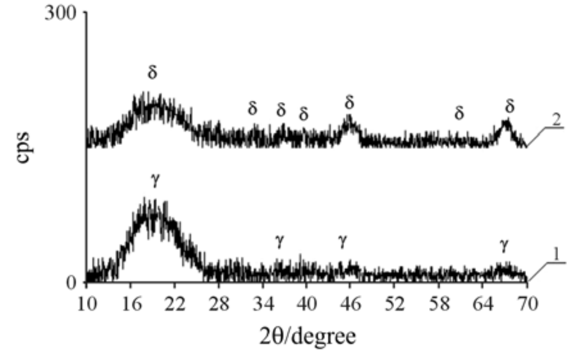

Fig. 3b XRD patterns of the products of calcination at 550 and 900°C of the sample AlOOH\0 h, 1 – AlOOH\0 h\550°C, 2 – AlOOH\0 h\550°C\900°C

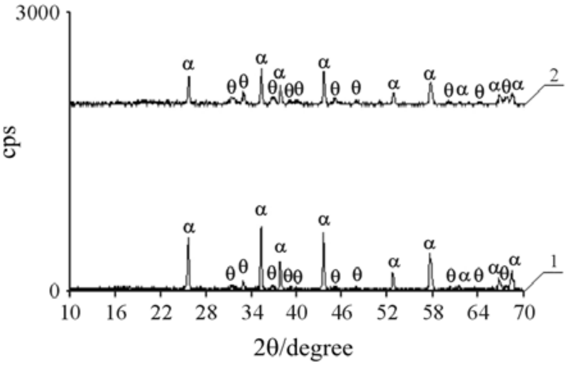

Fig. 3c XRD patterns of the products of calcination at 1200°C of the samples AlOOH\0 h and AlOOH\59 h,
1 – AlOOH\0 h\550°C\1200°C,
2 – AlOOH\59 h\550°C\1200°C

gous ones recorded for aluminium hydroxide aged for 59 h and oxides derived from it, as it was noticed in the case of materials prepared from aluminium chloride and perchlorate [4, 5].

The character change of the patterns resulted from the calcination of the samples at higher and higher temperature (550, 900 or 1200°C) confirms the sequence of transitions of aluminium hydroxide into a thermodynamically stable α phase, which was suggested on the basis of the IR studies.

The XRD spectra for both hydroxides reveal peaks characteristic for boehmite (Fig. 3a) [20, 21]. The character of the patterns makes it possible to suppose that apart from boehmite structure the samples also contained pseudoboehmite, as the term of ‘pseudoboehmite’ refers to a poorly crystallised boehmite whose low crystallinity degree is reflected in a considerable broadness and weak intensity of the peaks typical of boehmite. In the case of aged hydroxides, the peaks are sharper and stronger (Fig. 3a), which proves a larger amount of boehmite in them in comparison with the hydroxide not subjected to ageing, and evidences a favourable influence of the ageing process on the formation of boehmite structure. Above notice is consistent with the results obtained from infrared spectroscopy. Generally, the character of recorded XRD patterns proves that both hydroxide samples were rather highly amorphous. This is probably a consequence of ability of the acetate ion to form even weak complexes with hydrolyzed aluminium cation, due to which an interaction of the CH_3COO^- ion with a participate particle does not have only the simple attractive electrostatic character, as in the case of such anions as Cl^-, NO_3^- and ClO_4^-. Complexing with dissolved aluminium species and specific adsorption of the anion probably decrease the surface charge and potential of particles resulting in a reduction of interparticle repulsion and loss of colloidal stability. This leads to an acceleration of aggregation and sedimentation processes, and thus, to a poorly crystalline product. Moreover, the formation of the CH_3COOH molecules as a result of an interaction between CH_3COO^- and H^+ in aqueous medium, strongly displaces equilibrium of hydrolysis in the direction of aluminium hydroxide precipitation, which additionally accelerates the process and favours a low crystallinity degree of the precipitate.

A character of the XRD patterns recorded for the products of calcination at 550°C of both hydroxides is typical for the structure of γ-Al_2O_3 (Fig. 3b) [20, 22–25]. An increase of calcination temperature up to 900°C resulted in the formation of subsequent transition alumina. The spectra of both aluminium oxides reveal peaks characteristic for δ-Al_2O_3 [22, 23, 26]. However, a detailed analysis of the spectra of aluminium oxides obtained at 550 and 900°C is rather difficult due to low crystallinity of these samples. A further increase of heating temperature to 1200°C led to the next phase transition resulting in the mixture of θ- and α-Al_2O_3 (Fig. 3c). Comparing the XRD patterns for both aluminium oxides one may notice that the peaks attributed to α-Al_2O_3 are less intensive, while the peaks associated with the θ form – stronger, in the case of the sample derived from the hydroxide subjected to ageing. It confirms the fact that the process of prolonged refluxing at elevated temperature promoted a delayed formation of a corundum structure and is consistent with the results of IR spectroscopy. Probably, during this process, a number of surface defects was decreased, which in consequence limited an ion diffusion and retarded sintering of particles while calcination [20]. The analogous conclusion was drawn in the case of the samples prepared from $AlCl_3$ and $Al(ClO_4)_3$ [4, 5].

Low-temperature nitrogen adsorption

Table 2 presents the values of specific surface determined by means of the method of low-temperature nitrogen adsorption for the products of hydrolysis, both not aged and aged for different time intervals (20, 39 or 59 h), as well as the samples obtained through their calcination at 550, 900 or 1200°C for 2 h.

The analysis of the data collected in Table 2 shows that precipitated aluminium hydroxides were characterised with high values of specific surface (261–279 $m^2\ g^{-1}$) – higher than the samples prepared in an analogous way from aluminium chloride and perchlorate [4, 5]. The sample of freshly precipitated hydroxide had the highest S_{BET}. All hydroxides subjected to ageing had lower values of specific surface area, and as it can be seen the values were lower and lower when the ageing time was longer and longer.

Table 2 Porous structure parameters for selected samples determined by low-temperature nitrogen adsorption and adsorption-desorption of benzene vapours

Sample	Specific surface (nitrogen)	Specific surface (benzene)		Surface of mesopores (Kisielev method)	
	S_{BET}/ $m^2\ g^{-1}$	$S_{BET\ (vertical)}$/ $m^2\ g^{-1}$	$S_{BET\ (planar)}$/ $m^2\ g^{-1}$	$S_{MEZ\ (adsorption)}$/ $m^2\ g^{-1}$	$S_{MEZ\ (desorption)}$/ $m^2\ g^{-1}$
AlOOH\0 h	279	335	209	178	256
AlOOH\0 h\550°C	252	193	121	173	232
AlOOH\0 h\550°C\900°C	148	142	89	107	143
AlOOH\0 h\550°C\1200°C	36	11	7	*	*
AlOOH\20 h	278	–	–	–	–
AlOOH\20 h\550°C	246	–	–	–	–
AlOOH\20 h\550°C\900°C	169	–	–	–	–
AlOOH\20 h\550°C\1200°C	52	–	–	–	–
AlOOH\39 h	267	–	–	–	–
AlOOH\39 h\550°C	259	–	–	–	–
AlOOH\39 h\550°C\900°C	180	–	–	–	–
AlOOH\39 h\550°C\1200°C	56	–	–	–	–
AlOOH\59 h	261	284	177	207	322
AlOOH\59 h\550°C	248	264	165	322	324
AlOOH\59 h\550°C\900°C	161	153	95	93	111
AlOOH\59 h\550°C\1200°C	55	49	30	*	*

*lack of hysteresis loop

The process of ageing includes two mechanisms: structural rearrangement and Ostwald ripening. During the first period, the particles undergo a dramatic water loss according to a structural rearrangement mechanism. In the second period, the particles continue to lose water steadily but much more slowly. The two mechanisms occur simultaneously, but their kinetics is very different: in the first period, the structural rearrangement mechanism governs the process of ageing of the amorphous precipitate, whereas in the second period – Ostwald ripening controls the process. The structural rearrangement occurring as the first one liberates surface area and porosity within the texture of the particles. When the loss of water proceeds more slowly, the steadily growth of the crystallite size through Ostwald ripening leads to a continuous decrease of the specific surface area [27]. Lowering values of specific surface area prove that the structural rearrangement was over and the second mechanism of Ostwald ripening dominated. In the case of the samples obtained from $AlCl_3$, a continuous increase of S_{BET} was observed confirming a domination of the structural rearrangement mechanism [4], while in the case of the samples prepared with the use of $Al(ClO_4)_3$ the values of specific surface area firstly increased to a maximum value and then decreased, which proved that the ageing process passed from the first stage of rearrangement to the second one of Ostwald ripening [5]. Taking this fact into consideration one may come to a conclusion that kinetics of ageing is the fastest for the hydroxides obtained in the presence of acetate ions.

Calcination at 550, 900 or 1200°C of all hydroxides resulted in a decrease of specific surface development, similarly to the samples prepared from chloride and perchlorate salts. However, aluminium oxides obtained by heating at 550 or 900°C maintained relatively high values of S_{BET}, from 246 to 259 $m^2\ g^{-1}$ for the samples calcined at 550°C, and from 148 to 180 $m^2\ g^{-1}$ for the samples heated at 900°C. Such high values of specific surface are typical of metastable aluminium oxides, whose formation was proved with the results of IR spectroscopy and X-ray powder diffraction. There are no distinct differences in the values for aluminium oxides obtained through heating at 550°C of not aged aluminium hydroxide and for oxides derived from hydroxides subjected to ageing for varying time intervals. Instead, in the case of aluminium oxides prepared at 900°C, the S_{BET} value determined for the sample obtained without the ageing step is audibly lower than the values for the oxides obtained in an analogous way, however taking into account the process of ageing. Thus, it may be supposed that prolonged refluxing of precipitated aluminium hydroxides in mother liquors and at elevated temperature favoured a higher thermal stability of prepared transition aluminium oxides.

Pore closure and/or pore coarsening accompanying the process of sintering at the temperature of 1200°C resulted in destroying of internal porosity of aluminium oxide particles, which was reflected in a decrease of specific surface development (S_{BET}=36–65 m^2 g^{-1}). Nevertheless, it can be noticed that the samples prepared from aged hydroxides had distinctly higher values of specific surface in relation to the analogous sample derived from the hydroxide not subjected to ageing. It confirms the conclusion drawn on the basis of the IR and XRD analyses that in the case of using aluminium acetate as a precursor of aluminium oxides, the process of prolonged ageing of precipitated hydroxides increases thermal stability of final oxides. Nevertheless, lengthening its duration from 20 to 59 h did not give any audible effect appearing in changes of specific surface area values.

Adsorption and desorption of benzene vapours

The exemplary adsorption and desorption isotherms of benzene vapours obtained for the product of hydrolysis not subjected to the process of ageing, as well as for the oxides derived from this sample are shown in Fig. 4. Figures 5a and b present the distribution of mesopore surface as a function of effective radii determined by the Dollimore-Hill's method with an assumption of the model of cylindrical pores open from both sides, for quartz as the adsorption layer, obtained for the products of hydrolysis (not aged and aged for 59 h) and the samples of oxides obtained from them at 550 and 900°C. The parameters of the porous structure of these materials are revealed in Table 2.

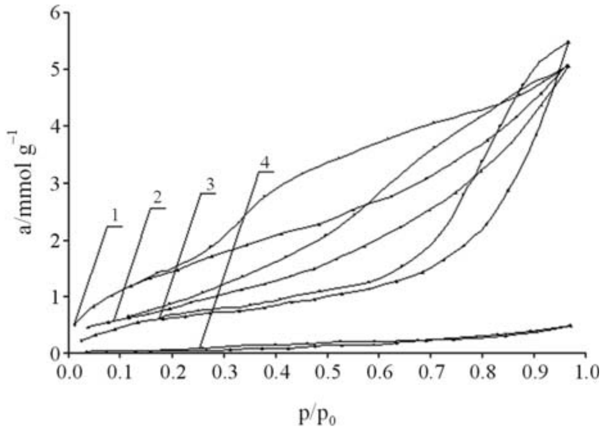

Fig. 4 The adsorption-desorption isotherms of benzene vapours for the sample AlOOH\0 h and products of its calcination at 550, 900 or 1200°C for 2 h,
1 – AlOOH\0 h, 2 – AlOOH\0 h\550°C,
3 – AlOOH\0 h\550°C\900°C,
4 – AlOOH\0 h\550°C\1200°C

The shape of isotherms obtained for both products of hydrolysis, as well as aluminium oxides calcined at 550°C may be classified according to IUPAC nomenclature as the H2 type [28]. Such a hysteresis loop corresponds to pores with shape resembling an 'inkstand' and to spherical pores open from both ends with significant inside necks. Instead, the shape of isotherms obtained for aluminium oxides calcined at 900°C may be classified as the H3 type [28]. For the materials of this kind, a hysteresis loop is qualified by capillary condensation between two layers, as a consequence of which bottle shape pores predominate in these samples. In the case of aluminium oxides heated at 1200°C the isotherms become flattened and narrowed, and the hysteresis loops disappear which is the evidence of low adsorption capacity of these samples.

The values of specific surface presented in Table 2, show that both hydrolysis products had good sorption capacity for benzene vapours, which is evidenced by high values of S_{BET} (Table 2) and high placed hysteresis loops (the exemplary Fig. 4). The character of changes of the S_{BET} values determined by means of the 'benzene' method arising from keeping the hydrolysis product in mother liquor at elevated temperature is consistent with the changes of S_{BET} values obtained with the method of low-temperature nitrogen adsorption i.e. a decrease of the S_{BET} value during the ageing process is observed (compare data in Table 2). Lower values for the hydrolysis product aged for 59 h in comparison with the sample not subjected to ageing, perhaps resulted from recrystallisation processes accompanying Ostwald ripening and leading to particle growth and reduction of intergranular space.

The process of calcination at 550–900°C led to a decrease of the S_{BET} values. Nevertheless, obtained aluminium oxides were characterised with a developed mesopore structure, which was confirmed by wide hysteresis loops and high values of mesopore surface determined by means of the Kisielev method, especially for the samples heated at 550°C (Table 2 and Fig. 4). Aluminium oxides calcined at 1200°C had significantly lower adsorption capacity for benzene vapours, which was evidenced by vanishing or emphatic narrowing of hysteresis loop, the lowest placed adsorption isotherms, and in consequence, low values of specific surface area. However, the sample prepared from hydroxide subjected to prolonged refluxing in mother liquor at elevated temperature had about four times higher values of $S_{BET\ (planar)}$ and $S_{BET\ (vertical)}$ than the values obtained for the sample prepared without the ageing step. This proves its higher thermal stability and is additionally confirmation for the results of the IR and XRD analyses, as well as for the results of low-temperature nitrogen adsorption.

A comparative analysis of nitrogen and benzene adsorption results gives the possibility of estimating the hydrophilic-hydrophobic properties of aluminium hydroxides and oxides [29, 30]. These properties depend on the surface functional groups that may alter the orientation of adsorbed benzene molecules and change the degree of their packing in the adsorption layer. The nitrogen molecule (inert gas) has a small seating surface (0.16 nm^2) as compared with that of benzene molecule (0.25 nm^2 in the vertical orientation and 0.40 nm^2 in the planar orientation). For this reason, if the surface structure is favourable for the planar orientation of benzene molecule, the specific surface $S_{\mathrm{BET\ (planar)}}$ should be smaller or equal to the S_{BET} value determined from the adsorption of nitrogen. Excessive values of $S_{\mathrm{BET\ (planar)}}$ with respect to the specific surface values determined from nitrogen adsorption may be accounted for the decrease of the seating surface of benzene molecule, which can be a result of the change of its orientation in adsorption layer. The deviation of benzene molecules on the surface of hydroxides and oxides is likely to be caused by surface hydroxyl groups.

For both products of hydrolysis (aged for 0 or 59 h) the $S_{\mathrm{BET\ (planar)}}$ values were higher than S_{BET} calculated with the ‘nitrogen’ method, which points to their hydrophilic properties. However, the process of ageing resulted in weakening of the hydrophilic character, similarly to the samples prepared with the use of $Al(ClO_4)_3$, and contrary to the materials obtained from $AlCl_3$. During a prolonged keeping of precipitated aluminium hydroxide in mother liquor, condensation of hydroxyl groups took place leading to removal of water molecules. Smaller amount of OH groups favoured planar orientation of benzene molecules. This explains closer values of S_{BET} and $S_{\mathrm{BET\ (planar)}}$ and weaker hydrophilic character.

Disappearing of divergences between the S_{BET} and $S_{\mathrm{BET\ (planar)}}$ values was also a consequence of the process of calcination at 550–1200°C. Aluminium hydroxides, during heating at high temperatures, underwent dehydroxylation, which was reflected in reinforcing their hydrophobic properties. Except the aluminium oxides obtained through calcination at 550°C of the hydroxide aged for 59 h, which possessed a slight hydrophilic character, all other oxides were characterized with definitely hydrophobic properties appearing in higher values of S_{BET} than $S_{\mathrm{BET\ (planar)}}$ and $S_{\mathrm{BET\ (vertical)}}$. Moreover, higher values of specific surface area determined by means of low-temperature nitrogen adsorption in relation to S_{BET} calculated with the ‘benzene’ method supposing both planar and vertical orientation of benzene molecule also pointed to a significant distance from particular benzene molecules in the adsorption layer and so, to a considerable rarefaction of the adsorption film. It is probable that in the case of these materials, a localised adsorption on unsaturated aluminium cations took place.

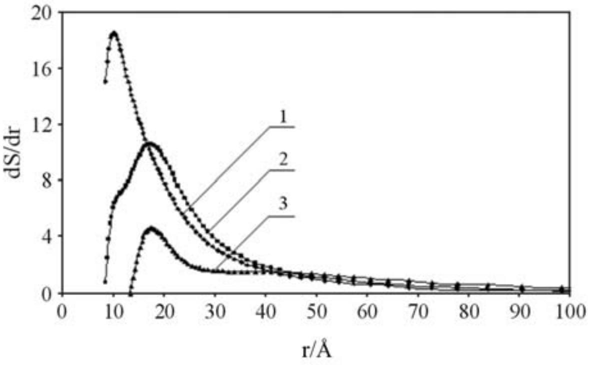

Fig. 5a The distribution of mesopore surface area as a function of the effective radii for the sample AlOOH\0 h and products of its calcination at 550 or 900°C for 2 h, 1 – AlOOH\0 h, 2 – AlOOH\0 h\550°C, 3 – AlOOH\0 h\550°C\900°C

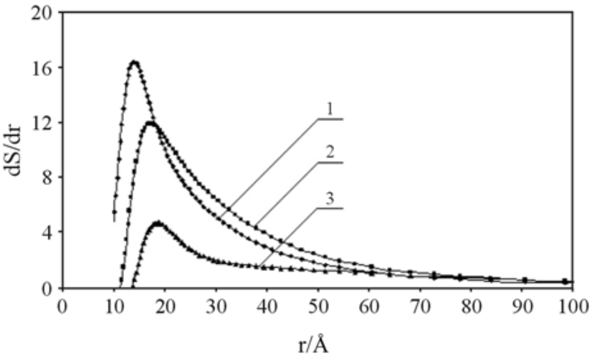

Fig. 5b The distribution of mesopore surface area as a function of the effective radii for the sample AlOOH\59 h and products of its calcination at 550 or 900°C for 2 h, 1 – AlOOH\59 h, 2 – AlOOH\59 h\550°C, 3 – AlOOH\59 h\550°C\900°C

Both products of hydrolysis of aluminium aceate (not aged and aged for 59 h) were characterised with monodispersive distribution of mesopore surface area as a function of effective radii (Figs 5a and b). It can be observed that the pores of radii of about 11–15 Å contributed to their porosity the most. In the case of the sample kept in mother liquor, a slight shift of the maximum in the direction of higher values is observed. An increase of the pore radii may be associated with removal of water molecules as a result of condensation of both surface and/or interlayer hydroxyl groups which is usually accompanied by liberation of free space; as well as with particle growth.

The samples obtained at 550 or 900°C were also characterised with monodispersive distribution of mesopore surface area as a function of effective radii

(Figs 5a and b). The calcination process carried on at 550 or 900°C caused the formation of slightly bigger pores with radii within 16–19 Å, which was probably a consequence of dehydroxylation taking place during calcination of the samples. Rising of heating temperature was not audibly reflected in an increase of contribution of pores with bigger radii.

Scanning electron microscopy

Figures 6a and b show exemplary microscopic photographs of the product of hydrolysis not subjected to ageing and the aluminium oxide obtained by its heating at 1200°C for 2 h, respectively.

All materials prepared during hydrolysis of aluminium acetate were milky-white precipitates which after drying became dusty powders easy to grind. They were characterised with a fine grained morphology visible in Fig. 6a. The representative photo taken with the magnification of ×500 shows that the materials were composed of spherical particles of the size not bigger than 1 μm which formed loose flocculent agglomerates homogeneous in size. The particles seemed to be a bit smaller than these obtained from aluminium chloride and perchlorate [4, 5]. A precipitate consisted of small particles was obtained in the presence of the CH_3COO^- ion also by researchers [31]. Complexing ability of acetate anion, stronger then in the case of chloride and perchlorate ions, could be the possible reason of small size of the grains. However, it should be underlined that opinions concerning the influence of an anion affinity toward hydrolyzed aluminium cation on the size of aluminium hydroxide particles are inconsistent. For instance, authors of papers [31–33] are of the opinion that chelating agents prevent Al^{3+} and OH^- from too fast nucleation which enables the separation of the nucleation and growth stages. Because of the fact that only a small amount of Al^{3+} is consumed in the nucleation, relatively large particles can be obtained. On contrary, researchers [16] think that due to strong affinity toward hydrolyzed aluminium cation, some anions may retard or make impossible the process of hydrolysis of polymeric Al–OH forms, as well as the process of their further polymerization leading to the formation of large particles.

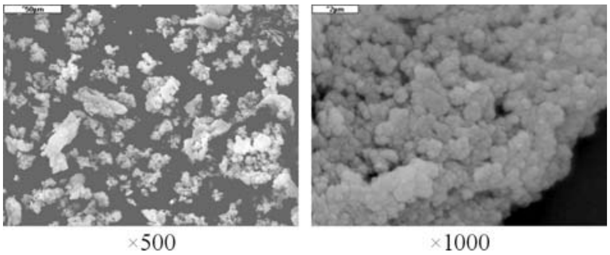
×500 ×1000

Fig. 6a SEM photographs for the product of hydrolysis not subjected to ageing

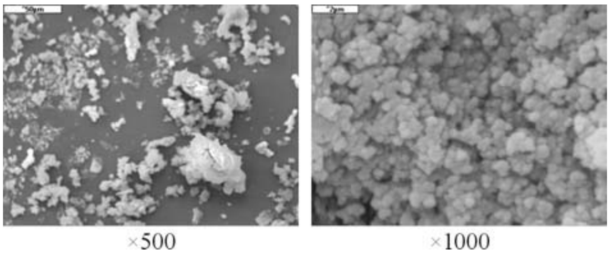
×500 ×1000

Fig. 6b SEM photographs for the product of calcination at 1200°C for 2 h of the sample AlOOH\0 h

Despite a small size of the grains, the products of hydrolysis of aluminium acetate displayed quite high thermal stability, which was proved with the IR and XRD analyses, as well as with low-temperature nitrogen adsorption and adsorption/desorption of benzene vapours. It is highly probable that the heat resistance of the materials was favoured by their specific morphology, i.e. spherical shape of particles forming loose aggregates of nearly equal size. The morphology of the hydrolysis products remained rather unchanged while their keeping in mother liquors at elevated temperature. In the case of the sample aged for 59 h, only a slight growth of the grains was noticed.

Similarly to materials prepared from $AlCl_3$ and $Al(ClO_4)_3$, calcination at 1200°C carried on for both products of hydrolysis of aluminium acetate did not result in considerable changes of morphology (the exemplary Fig. 6b). Heating at high temperatures caused slow sintering and coarsening of the grains; however, in the photo taken with the magnification of ×10000 there are still many loose individual particles. No distinct differences in the morphology of the oxides derived from not aged hydroxide and the hydroxide subjected to ageing for 59 h were observed.

Conclusions

- The hydrolysis of aluminium acetate in ammonia medium results in the formation of the mixture of boehmite and pseudoboehmite.
- Prolonged refluxing of freshly precipitated aluminium hydroxide develops its crystallinity, decreases its specific surface determined from nitrogen adsorption and sorption capacity for benzene vapours, as well as diminishes its hydrophilic character.
- Extending of ageing duration (from 20 to 59 h) has a slight effect on the properties of hydroxides.
- Obtained aluminium hydroxides during calcination at temperature up to 1200°C transform to α-Al_2O_3 via γ-, δ- and θ-Al_2O_3.

- The samples of aluminium oxides obtained after calcination at 550 and 900°C are characterised with high values of specific surface area of 246–259 and 148–180 $m^2 g^{-1}$, respectively.
- Obtained transition aluminium oxides displayed high heat resistance, probably due to a specific morphology of starting aluminium hydroxides.
- The process of ageing at elevated temperature develops thermal stability of aluminium oxides.

References

1 S. Ramanathan, S. K. Roy, R. Bhat, D. D. Upadhyaya and A. R. Biswas, Ceram. Int., 23 (1997) 45.
2 J. Temuujin, Ts. Jadambaa, K. J. D. Mackenzie, P. Angerer, F. Porte and F. Riley, Bull. Mater. Sci., 4 (2000) 301.
3 S. Ramanathan, S. K. Roy, R. Bhat, D. D. Upadhyaya and A. R. Biswas, J. Alloys Compd., 243 (1996) 39.
4 B. Pacewska, O. Kluk-Płoskońska and D. Szychowski, J. Therm. Anal. Cal., OnlineFirst, DOI:10.1007/s10973-005-7016-x.
5 B. Pacewska, O. Kluk-Płoskońska and D. Szychowski, J. Therm. Anal. Cal., OnlineFirst, DOI:10.1007/s10973-005-7377-1.
6 B. Pacewska, O. Kluk-Płoskońska and D. Szychowski, Influence of Aluminium Precursor on Physico-Chemical Properties of Aluminium Hydroxides and Oxides. Part III–$Al_2(SO_4)_3$–$18H_2O$, J. Therm. Anal. Cal., (2006) – submitted.
7 B. Pacewska, D. Szychowski and T. Żmijewski, Computer program for evaluation of parameters of porous structure of solids, Forum Chemiczne 2000, Warszawa 200.
8 X. Bokhimi, J. A. Toledo-Antonio, M. L. Guzmán-Castillo, B. Mar-Mar, F. Hernández-Beltrán and J. Navarrete, J. Solid State Chem., 161 (2001) 319.
9 J. T. Kloprogge, J. W. Geus, J. B. H. Jansen and D. Seykens, Thermochim. Acta, 209 (1992) 265.
10 S. Desset, O. Spalla, P. Lixon and B. Cabane, Colloids Surf. A, 196 (2002) 1.
11 J. J. Fripiat, H. Bosmans and P. G. Rouxhet, J. Phys. Chem., 71 (1967) 1097.
12 R. L. Frost, J. Kloprogge, S. C. Russell and J. L. Szetu, Thermochim. Acta, 329 (1999) 47.
13 E. Ingier-Stocka, C. Mazanek, L. Rycerz and R. Wojciechowska, Wodorotlenki i tlenki glinu. Właściwości i technologia ich otrzymywania, Wydawnictwo Politechniki Wrocławskiej, Wrocław 1984, p. 8.
14 C. Morterra and G. Magnacca, Catal. Today, 27 (1996) 497.
15 S. Musić, Đ. Dragčević, S. Popović and N. Vdović, Mater. Sci. Eng., B 52 (1998) 145.
16 S. Musić, Đ. Dragčević, S. Popović and N. Vdović, Mater. Chem. Phys., 59 (1999) 12.
17 J. T. Kloprogge and R. L. Frost, Spectrochim. Acta, Part A, 55 (1999) 163.
18 J. van den Brand, S. van Gils, P. C. J. Beentjes, H. Tercyn and J. H. W. de Wit, Appl. Sci. Surface, 235 (2004) 465.
19 P. Person, M. Karlsson and L.-O. Öhman, Geochim. Cosmochim. Acta, Vol. 62, No. 23/24 (1998) 3657.
20 G. K. Chuagh, S. Jaenicke and T. H. Xu, Microporous Mesoporous Mater., 37 (2000) 345.
21 S. D. Vaidya and N. V. Thakkar, J. Phys. Chem. Solids, 62 (2001) 977.
22 K. Okada, T. Nagashima, Y. Kameshima and A. Yasumori, J. Colloid Interface Sci., 248 (2002) 111.
23 K. T. Hwang, H. S. Lee, S. H. Lee, K. C. Chung, S. S. Park and J. H. Lee, J. Eur. Ceram. Soc., 21 (2001) 375.
24 Y. Kim, Ch. Kim, P. Kim and J. Yi, J. Non-Cryst. Solids, 351 (2005) 550.
25 E. E. Kiš, G. A. Lomić, G. C. Bošković and R. P. Marinković-Nedučin, React. Kinet. Catal. Lett., 63 (1998) 323.
26 X. Wang, G. Lu, Y. Gou, Y. Wang and Y. Guo, Mater. Chem. Phys., 90 (2005) 225.
27 J. M. Rousseaux, P.Weisbecker, H. Muhr and E. Plasari, Ind. Eng. Chem. Res., 41 (24) (2002) 6059.
28 IUPAC Reporting Physisorption Data, Pure Appl. Chem., 57 (1985) 603.
29 B. Pacewska and D. Szychowski, Przem. Chem., 48 (3) (2006) 171.
30 B. Pacewska and D. Szychowski, J. Therm. Anal. Cal., 80 (2005) 687.
31 J.-Y. Park, S.-G. Oh, U. Paik and S.-K. Moon, Mater. Lett., 56 (2002) 429.
32 J. L. Shi, J. H. Gao and Z. X. Lin, Solid State Ionics, 32/33 (1989) 537.
33 M. Yada, H. Hiyoshi, M. Machida and T. Kijima, J. Porous Mater., 5 (1998) 133.

Received: September 20, 2006
Accepted: November 15, 2006
OnlineFirst: April 29, 2007

DOI: 10.1007/s10973-006-8202-1